scientific reports

Check for updates

OPEN

Higher dominant muscle strength is mediated by motor unit discharge rates and proportion of common synaptic inputs

Edoardo Lecce[1,3], Alessandro Del Vecchio[2,3], Stefano Nuccio[1], Francesco Felici[1] & Ilenia Bazzucchi[1]✉

Neural determinants explaining the asymmetrical force and skill observed in limb dominance still need to be comprehensively investigated. To address this gap, we recorded myoelectrical activity from biceps brachii using high-density surface electromyography in twenty participants, identifying the maximal voluntary force (MVF) and performing isometric ramp contractions at 35% and 70%MVF and sustained contractions at 10%MVF. Motor unit discharge characteristics were assessed during ramp contractions, the proportion of common synaptic input to motoneurons was calculated with coherence analysis, and the firing rate hysteresis (ΔF) was used to estimate spinal motoneuron intrinsic properties. The dominant limbs presented a greater MVF compared to the non-dominant side (+9%, $p = 0.001$), with similar relative recruitment and derecruitment thresholds of motor units ($p > 0.05$). The discharge rate was significantly higher on the dominant side ($p < 0.001$), along with a greater proportion of common synaptic input (+14%, $p = 0.002$). No significant differences were observed in the ΔF ($p > 0.05$). Our findings suggest that greater strength on the dominant side is associated with higher neural drive to muscles due to a greater proportion of common synaptic inputs rather than differences in motoneuron intrinsic properties. These results underscore neural asymmetries at the motor unit level, corresponding to different mechanical outputs underlying limb dominance.

Limb dominance is recognized as the preferential strength and skill within a single limb, implying asymmetrical neuromuscular control. While between-limb differences in gross motor properties, such as limb strength, the symmetry index, and balance, have been broadly investigated in various muscle groups[1], the underlying physiological mechanisms contributing to these disparities remain relatively underexplored. Researchers have sought to elucidate the primary neuromuscular properties contributing to this phenomenon with numerous and heterogeneous results, spanning from differential motor unit discharge synchronization impacting force steadiness[2], the influence of corticospinal neuron involvement in simple tasks, which is greater in the non-dominant hands[3], and the different intra-muscle synergies involved in simple and complex tasks[4].

Previous surface electromyography (sEMG) results revealed no limb differences in motor unit recruitment for the biceps brachii (BB)[5]. Evidence also indicates wider sEMG signal amplitudes in the pectoralis major, anterior deltoid, and triceps brachii on the dominant side across different contraction intensities[6]. Nevertheless, conflicting findings concerning motor unit discharge characteristics have been reported. It has been indicated that tibialis anterior (TA) from both sides present a similar discharge rate explored with high-density surface electromyography (*HDsEMG*)[7]. However, lower motor unit discharge rates[8] and recruitment thresholds in the first dorsal interosseus (FDI) have been observed on the dominant side[9]. It is also unclear whether dominant and non-dominant limbs present significant differences in force steadiness, as the FDI seems to exhibit more steadiness on the dominant side[9], whereas comparable force steadiness has been found in TA[7,10] and quadriceps[11].

Previous research has highlighted greater common synaptic input in the dominant lower limb muscles[12], while an opposite trend has been observed in hand muscles, with a similar proportion of common synaptic input during isometric contractions and even less common input on the dominant side during isometric rotational tasks[13]. Such differences may result from the differential distribution of common synaptic inputs between muscle groups, as well as the flexible coordination required for fine motor tasks implicating either or both a

[1]Laboratory of Exercise Physiology, Department of Movement, Human, and Health Sciences, University of Rome "Foro Italico", Rome, Italy. [2]Department Artificial Intelligence in Biomedical Engineering, Faculty of Engineering, Zentralinstitut für Medizintechnik (ZIMT), Friedrich-Alexander University Erlangen-Nürnberg, Erlangen, Germany. [3]E. Lecce and A. Del Vecchio contributed equally to this work. ✉email: ilenia.bazzucchi@uniroma4.it

lower proportion of common input and multiple sources of common input[14–16]. Distinct laterality of neural networks supporting actions in right and left-handed participants, indicating significant differences between these individuals[17] and between the dominant and non-dominant sides[18] have also been suggested in previous evidence.

The abovementioned findings lay the groundwork for different suggestions: *i*) motoneurons receive different proportions of common synaptic inputs based on the muscle and task; *ii*) distinctive laterality of neural networks may suggest a differential organization of motor patterns likely reflected in the motor unit discharge and recruitment behavior [limiting factor: it seems that network laterality is dependent on handedness rather than limb-dominance]; and *iii*) further differences may emerge from the analyses within the other frequency bandwidths accompanying plausible dominance in the force steadiness. To test these hypotheses, we assessed motor unit characteristics and estimates of the proportion of common synaptic inputs to motoneurons by recording myoelectrical activity from the biceps brachii on both sides, as no studies have currently investigated this muscle for this purpose. Furthermore, since the contribution of the intrinsic motoneuron properties to limb dominance is underexplored, we estimated the persistent inward currents (PICs) using recordings obtained with high-density surface EMG (HDsEMG)[19,20]. By integrating these approaches, we aim to explore motor unit determinants underlying limb dominance with a comprehensive analysis.

Based on existing literature[8,9,12,17], we expected to observe on the dominant side: (*a*) higher discharge rates, (*b*) a greater proportion of common synaptic inputs, and (*c*) larger PICs. Additionally, we hypothesized greater absolute recruitment and derecruitment thresholds in the dominant limbs, as these typically exhibit higher maximal force outputs[1].

Methods

Participants and ethical approval

The study was approved by the local ethical committee of the University of 'Foro Italico,' Rome (Approval n. CAR157/2023) and conformed to the *Declaration of Helsinki* standards. Twenty-three recreationally active participants were enrolled (males: $n = 11$, age: 24.1 ± 1.1 years, height: 178.2 ± 5.4 cm, body mass index [BMI]: 24.1 ± 2.5 m kg^{-2}; females: $n = 12$, 24.3 ± 2.2 years, height: 164.9 ± 5.5 cm, BMI: 19.9 ± 2.0 m kg^{-2}) and assigned unique alphanumeric codes to ensure privacy respect and confidentiality. Informed consent was obtained from all the participants. The exclusion criteria included metabolic disease, upper limb musculoskeletal disorders, acute infection, uncontrolled hypertension, medications that impact muscle protein metabolism, the ability to modulate vascular tone and neural activity, and the use of contraceptives[21]. The inclusion criteria were an age between 18 and 35 years and a good health state.

Overview of the study

The participants were asked to be available for two laboratory visits, the first for familiarization and the second for the neuromuscular tests and data collection, which were separated by 48–72 h. During the first visit, volunteers received information on experimental and testing procedures. They were familiarized with maximal voluntary isometric contractions (MVICs), sustained contractions, and trapezoidal isometric contractions (ramps) using the biceps brachii, and the dominant limb was identified using the Edinburgh Questionnaire[22]. No measurements were performed during the familiarization. Data were acquired during the second visit, including maximal voluntary force (MVF) and submaximal ramp contractions. High-density surface electromyography (HDsEMG) grids were placed on the biceps brachii, and the myoelectrical activity of both limbs was recorded, one limb at a time. Female participants performed the test during either the ovulatory or mid-luteal phase to reduce neuromuscular activity fluctuations and to avoid a documented decrease in general activation attributed to the early follicular phase. This approach ensures minimal motor unit parameter variability across female participants[23]. Dominant and non-dominant limbs were randomly assessed within the session across participants.

Experimental procedures

The volunteers were asked to refrain from strenuous exercise and caffeine consumption 24–48 h before the tests[24]. The arm circumference and subcutaneous skinfold thickness (SST) were assessed to verify whether the expected differences in force output could be attributed to muscle size. Each measurement was performed three times, and the average value was used to ensure accuracy. The neuromuscular test was performed after a standardized warm-up, consisting of 3×30 isometric biceps brachii contractions at a low intensity of the perceived MVF (30–40% MVF) separated by 30 s. The participants were asked to focus on isolating the BB intervention as much as possible during the warm-up and testing procedures. Consequently, the participants performed three MVICs with 180 s of rest between trials, and they were asked to push as hard as possible for 5 s, receiving a strong verbal incitation to ensure maximal focus for all trials[24]. The MVF was identified as the peak value recorded across the three MVICs to set the relative target force (%MVF) in submaximal contractions. Five minutes after the last maximal trial, the participants performed ramp contractions in a randomized order separated by 5 min. The ramps consisted of a linear force increase at a rate of 5% MVF s^{-1} to a target value (35% or 70% MVF), which was maintained for 10 s; then, the linear force decreased back to the resting value at the same rate as the increasing phase. Sustained contractions at 10% MVF were performed five minutes after the last ramp contraction and lasted 1 min (Fig. 1A).

Force signal recording

The force output was assessed with an isokinetic dynamometer (Kin-Com, Chattanooga, Tennessee). The participants were seated in the dynamometric chair and stabilized by chest and waist belts. The upper arm was parallelly positioned to the trunk, and the forearm was halfway between supination and pronation, with

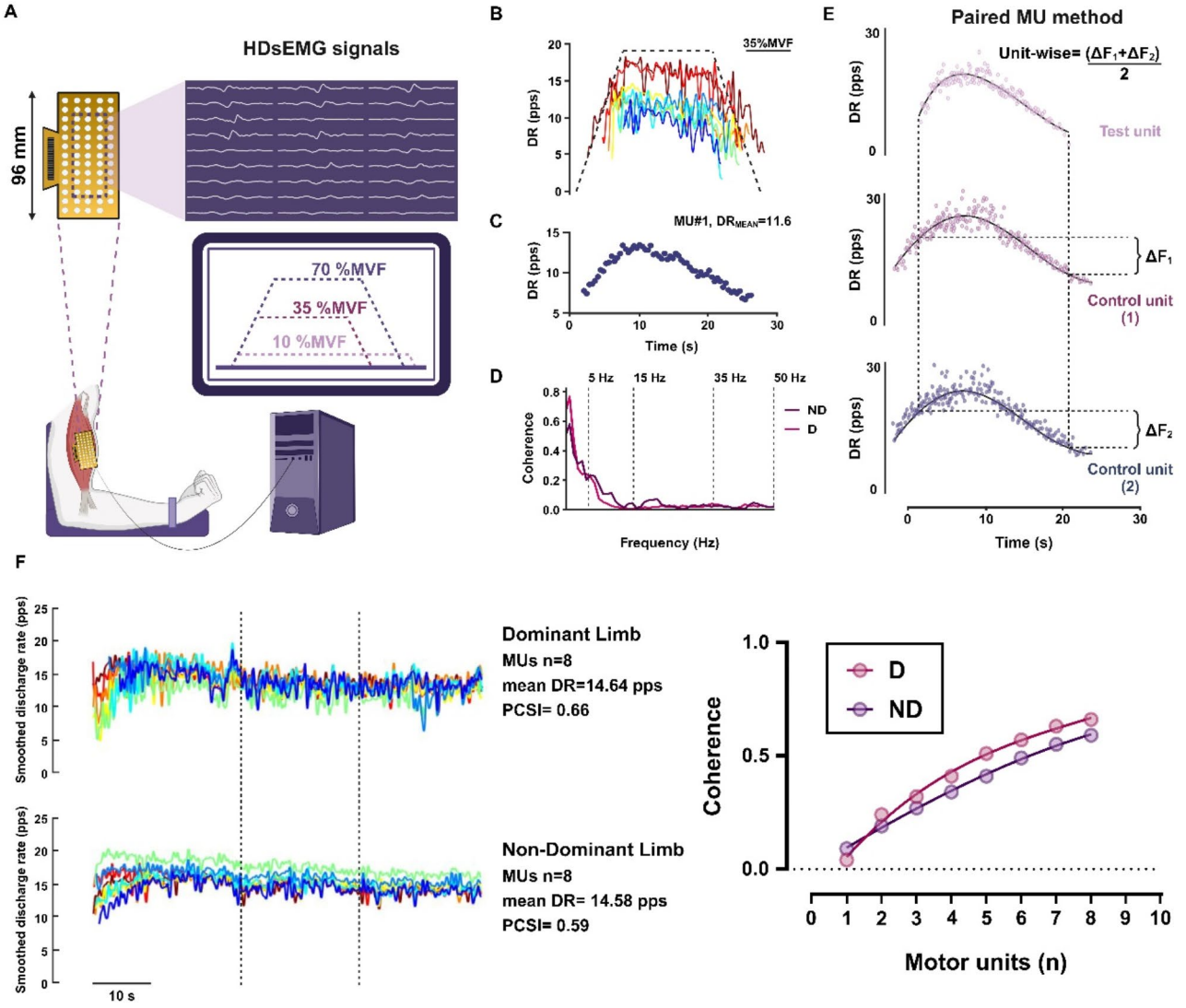

Fig. 1. Experimental setup. (**A**) HDsEMG recordings were obtained from participants' biceps brachii during trapezoidal (35-70% MVF) and sustained (10% MVF) contractions in visually guided tasks. The force trajectory was displayed on a monitor in real-time. (**B**) Cumulative discharge patterns were identified with the decomposition process for all motor units to obtain the smoothed discharge rate of single motor units, with 35% MVF as a representative contraction. (**C**) Instantaneous discharge rates of motor units across the task were identified to estimate discharge parameters, exemplified by motor unit 1 (MU#1) from the same 35% MVF contraction. (**D**) Coherence was estimated in sustained contractions using the frequency domain analysis. The delta (δ, 0–5 Hz), alpha (α, 5–15 Hz), and beta (β, 15–35 Hz) bandwidths were identified. (**E**) The paired motor unit method was used to assess the firing rate hysteresis by calculating the difference between the control unit discharge rate at recruitment and derecruitment time of the tested unit (ΔF) from pairs of identified motor units. The earliest recruited unit is classified as the control unit, whereas the other is the tested unit. The unit-wise value was calculated by summing multiple ΔF results from more possible pairs and dividing by the number of ΔF included. (**F**) Coherence was calculated with non-overlapping 1-s Hanning windows within the central 20-s interval. This process involves correlating multiple pairs of motor unit spike trains from all the possible combinations (a maximum of 100 random permutations). An equal number of motor units was ensured for between-limb comparisons. Coherence increased consistently with the inclusion of more motor units, with each step leading to higher coherence values. This visual example highlights that different coherence values can arise from the discharge rate correlation, even when discharge rates and the number of motor units are similar. The image was realized with biorender.com.

elbow flexion of 90°. The distal lateral epicondyle of the humerus was aligned with the dynamometer lever arm center of rotation, and the wrist was secured in a cuff attached to the load cell, which consisted of four strain gauges. The analog force signal was sampled and amplified at 2048 Hz with an external analog-to-digital (A/D) converter (EMG-400, OT-Bioelettronica, Turin, Italy) and synchronized with the electromyogram. Since the

trapezoidal contractions needed to be visually guided, a trapezoidal pattern was shown to participants during the contraction, with a minimum/maximum error of 3% MVF (± 1.5% MVF).

High-density surface electromyography (HDsEMG)

HDsEMG signals were recorded from the BB with an adhesive grid of 64 electrodes [13 rows x 5 columns; gold-coated; diameter: 1 mm; inter-electrode distance (IED): 8 mm; OT-Bioelettronica, Turin, Italy; Fig. 1A]. After skin preparation (shaving, light skin abrasion, and 70% ethanol cleansing), the muscle perimeter was identified through palpation and marked with a surgical pen. The grid orientation was based on recordings from a 16-electrode array (IED 5 mm, OT-Bioelettronica, Turin, Italy), and the innervation zone (IZ) was identified to estimate the fiber direction[23]. The IZ was located by identifying the inversion point in the action potential propagation direction proximally (toward the BB proximal tendon) and distally (toward the BB distal tendons) along the electrode column. The grid was placed right over the IZ on the muscle belly, using a disposable biadhesive with layer holes adapted to the HDsEMG grids (SpesMedica, Battipaglia, Italy). The foam layer holes were filled with a conductive paste (SpesMedica, Battipaglia, Italy) to ensure skin-electrode contact. Reference electrodes were positioned on the ulna [styloid process], the acromion skin surface, and the medial malleolus. HDsEMG signals were recorded in monopolar mode, converted to digital data by a 16-bit multichannel amplifier (EMG-Quattrocento, OT Bioelettronica, Turin, Italy), amplified (x150), sampled at 2048 Hz, and band-pass filtered (10–500 Hz) before being stored for offline analysis.

Force and HDsEMG analysis

The recorded force signal was converted to newtons (N), and gravity compensation was used to remove the offset. The signal was low-pass filtered with a fourth-order, zero-lag Butterworth filter with a cut-off frequency of 15 Hz. Only trapezoidal contractions without any countermovement action or pre-tension were analyzed. Before decomposing into individual motor unit action potentials, the monopolar EMG recordings were band-pass filtered at 20–500 Hz (second-order, Butterworth). The raw HDsEMG signals were decomposed using the convolutive blind-source separation method [BSS][25] implemented in the DEMUSE tool software working in MATLAB (MathWorks Inc. Natick, United States). This decomposition procedure can identify motor unit discharge times over a broad range of forces (Fig. 1C,D)[26]. An experienced investigator manually analyzed all the identified motor units and retained only those characterized by a high pulse-to-noise ratio [PNR > 30 dB][27]. The manual analysis consists of inspection and editing procedures after automatic decomposition, involving examination of motor unit spike trains during the whole contraction, discarding those motor units with a PNR below the reference threshold following the manual process (30 dB), interspike interval of length < 25 ms or > 250 ms (instantaneous spike frequency > 40 Hz or < 4 Hz, respectively) or interspike interval variability (ISIv) > 30% to nsure maximal accuracy[26].

The recruitment and derecruitment thresholds (RT and DT, respectively) were identified as the absolute (N) and the relative (%MVF) force values at which motor units were activated and deactivated, identifying the first and the last spikes[26]. The average discharge rate was computed from the series of discharge times identified by decomposition, obtained by calculating the discharge number per second for each motor unit (DR_{MEAN}) across the entire activity time at all contraction intensities [10–35%–70% MVF]. The motor unit discharge rate was estimated during the recruitment (DR_R), plateau (DR_P), and derecruitment (DR_D) phases of ramp contractions by averaging four consecutive spike frequencies for each phase. The ISIv was assessed during the sustained phases in the ramp contractions [35%MVF–70%MVF] and the central 20-s of steady contractions [10%MVF]. Recruitment and dercruitment thresholds and the discharge rate at recruitment, plateau, and derecruitment were assessed only in trapezoidal contractions (35–70% MVF), as these have been validated for these analyses[26].

Since significant differences between groups may arise not from an inherent distinction in the limbs themselves but from the distribution of identified motor units expressing a specific characteristic across individuals[26], we characterized recruitment and discharge patterns by associating the derecruitment threshold and DR_P to the recruitment threshold, as previously indicated[23]. This approach enables a normalized analysis of recruitment and discharge patterns independent of the number of identified motor units, thereby allowing accurate comparisons between groups (i.e., between limbs).

The coefficient of variation of force (CoVF), defined as the percent ratio between the standard deviation and the mean force ([SD/mean] × 100), was calculated over the central 20 s of sustained contractions and the central 8 s portion of trapezoidal contractions discarding the first and the last 1-s period to minimize fluctuations due to the ramp-up/ramp-down transitions[27]. The limb symmetry index was calculated as follows: $\left(\frac{\text{non-dominant MVF}}{\text{dominant MVF}}\right)$ x 100, broadly used for comparing the balance degree in force production between limbs[1].

We additionally computed the association between the change in motor unit discharge rate (Δ-DR) as a function of the relative force exerted (Δ-Force) during the ramp-up phase of contractions, reflecting the motoneuron output response to synaptic input[28,29]. This analysis provides an indirect estimation of the motoneuronal input-output gain within a pool, reflecting the gain in motor unit discharge rate from activation to the target force, relative to the change in exerted force determined by all sources of input to spinal motoneurons, as previously indicated[23,28]. Specifically, the activation of a given motoneuron, supporting force exertion from a certain output level (recruitment as % MVF) to the target force, is supported by a varying synaptic input, which is transmitted as neural drive to muscles[30,31]. By computing the regression across the motoneuron pool, it is possible to indirectly estimate the input-output gain within motoneurons in the same individual as the change in neural drive in response to the estimated synaptic input[28,29,32]. Modifications in the input-output function imply differences in the gain of motoneurons when the system requires force generation, along with variations in the slopes of this function[19,28,29].

Coherence estimation

To estimate the level of common synaptic input, we performed the coherence analysis between cumulative spike trains of the motor units. Coherence represents the correlation between two signals at a certain frequency, with 0 indicating no correlation and 1 indicating perfect correlation[13]. This analysis was performed exclusively within the central 20-s window of the 1-min sustained contractions at 10% MVF, excluding the initial ramp-up portion[27], as the common modulation of motor unit discharge rate is generally lower during the recruitment but typically higher during steady contraction phases[33]. Indeed, motor units do not fire concurrently when asynchronously recruited, whereas a higher degree of correlation is observed when motor units fire together due to the shared synaptic input from the central nervous system[33]. This window was also selected as we found the maximum number of concurrently active units for most participants. Furthermore, coherence values are mathematically influenced by the motor unit discharge rate[34], as higher spike frequencies directly elevate coherence values. Currently, no methods are available to adjust for this dependency[33]. For each iteration (number of units), all the unique combinations of motor units were tested up to a maximum of 100 random permutations[35] and computed in all cases with non-overlapping 1-s Hanning windows on steady pattern of force exertion at a constant discharge rate.

Previous evidence demonstrated that the correlation between cumulative motoneuron trains of discharges increases monotonically with the number of motor unit spike trains used for calculations[36,37]. Thus, the function representing the coherence value as a function of the number of motor neuron spike trains is a monotonically increasing function (Fig. 1F). The rate of the increase in coherence depends on the proportion of common input relative to independent input, with a steeper increase when more common input is present[37]. Therefore, when a similar number of motor units are used for the estimation, differences in coherence represent differences in the strength of common input between these units[36]. An equal number of motor units must be analyzed to accurately compare dominant and non-dominant limbs[27]. This was achieved by excluding motor units with higher interspike interval variability (> 30%), lower pulse-to-noise ratios (< 30 dB), or abnormal discharge rate values (e.g., > 30 Hz at 10% MVF) within the identified pool following previous evidence[33,38]. Therefore, coherence calculations were performed using an equal number of motor units for each individual, ensuring that the same number of motor units was used for the dominant and non-dominant limbs within each participant (e.g., ID1: dominant limb, 5; non-dominant limb, 5; ID2: dominant limb, 4; non-dominant limb, 4). By doing so, only 17 participants satisfied these criteria.

Coherence values (C) were transformed into standard z-scores by first converting them into Fisher's values [FZ = atanh ($\sqrt{C}$)] and then normalized to the variance of estimation [Z = FZ / $\sqrt{1/2L}$] where L is the number of segments used to calculate coherence without overlapping (e.g., 20 windows of 1 s, L = 20). This process ensures the normalization of coherence results, conferring robustness and reliability of comparisons[13]. The estimated bias was identified as the mean z-coherence values within the 100–250 Hz range and subtracted from coherence functions where no coherence was expected[36], and significant coherence was considered when the z score was greater than 1.22 (95% confidence limit)[13]. Averaged values obtained within δ [delta, 0–5 Hz], α [alpha, 5–15 Hz], and β [beta, 15–35 Hz] frequency bandwidths were analyzed (Fig. 1B).

Paired-motor unit method

The persistent inward currents were estimated using motor unit onset-offset hysteresis (ΔF) from pairs of motor units identified by correlating their discharge rates[39]. The correlation was performed within consecutive 500-ms windows using the rate-rate correlation, which provides an index of common modulation of two concurrently active motor units. This process includes plotting the average discharge rate for each window in 500-ms bin[40] of both reference and test units for the duration of the ramp. Correlations with values less than $r = 0.7$ do not meet the assumption of shared synaptic input[40]. Hence, only motor unit pairs with $r > 0.7$ were considered for the analysis.

The observed discharge events for each motor unit were converted into instantaneous discharge frequencies and fitted with a fifth-order polynomial function[40]. The earliest recruited motor unit was designated as control, while the other was considered the test unit[39]. ΔF was calculated as the difference in the discharge rate of the control motor unit at the times of recruitment and derecruitment of the test motor unit (Fig. 1E). When more than two motor units were identified for possible pairs, this process included a calculation of the sum of ΔF divided by the number of pairs [e.g., three pairs = $(\Delta F_1 + \Delta F_2 + \Delta F_3)/3$] to obtain the *unit-wise*[41]. Thus, the same motor unit could be the reference for one pair and the tested for another. The present approach assumes that PICs in the reference unit are fully activated before the test motor unit is recruited, which has been reported to take up to 2 s in human motoneurons[19]. Therefore, the analysis did not consider possible motor unit pairs showing a difference in recruitment time < 2-s. In addition, a test unit must be derecruited at least 1.5-s before the reference unit for accurate calculations and not overestimate ΔF[41].

Although evidence based on simulation results has suggested that steady phases of contraction could affect the estimate of the PICs[42], recent in vivo research has consistently demonstrated that trapezoidal ramp contractions are highly reliable for estimating the persistent inward currents. These studies employed both iEMG and HDsEMG across various experimental conditions in a range of 10–40% MVF, confirming the robustness of both triangular and trapezoidal contractions with different plateau phase durations for this type of physiological assessment[40,41,43]. Calculating ΔF requires low-threshold motor units to approximate synaptic input, which is difficult to decompose successfully at higher contraction intensities due to the superimposition of larger, higher-threshold motor units in the HDsEMG signals[41]. Therefore, ΔF values obtained at the 70% MVF were not considered and are reported only for completeness of information in the result section.

	10%MVF	35%MVF	70%MVF	Total
D	125	136	93	354
ND	114	144	91	349
Total	239	280	184	703

Table 1. Distribution of identified motor units. No between-limb differences were observed in the number of identified motor units per participant.

	35%MVF			70%MVF		
	D	ND	P	D	ND	P
DR_{MEAN} (pps)	19.0 ± 4.7	17.0 ± 4.2	**< 0.001**	21.9 ± 5.9	18.9 ± 4.4	**< 0.001**
DR_R (pps)	14.5 ± 4.5	12.7 ± 3.8	**< 0.001**	14.8 ± 4.7	12.8 ± 4.0	**0.001**
DR_P (pps)	19.5 ± 4.9	17.9 ± 4.5	**0.003**	22.8 ± 5.7	20.5 ± 5.0	**< 0.001**
DR_D (pps)	11.6 ± 3.6	10.4 ± 2.6	**0.009**	13.9 ± 5.1	12.0 ± 3.8	**< 0.001**
ISIv (%)	23.6 ± 7.4	23.9 ± 7.2	0.764	28.6 ± 7.9	27.8 ± 8.0	0.483
RT (N)	80 ± 39	69 ± 30	**< 0.001**	148 ± 66	123 ± 57	**< 0.001**
DT (N)	68 ± 33	59 ± 29	**0.009**	147 ± 62	126 ± 57	**0.006**
RTr (%)	28.4 ± 5.9	26.7 ± 5.2	0.707	52.5 ± 10.8	47.9 ± 10.4	0.110
DTr (%)	24.1 ± 6.5	23.1 ± 6.8	0.876	52.0 ± 10.7	49.2 ± 8.9	0.882

Table 2. Myoelectrical parameters during ramp contractions. Significant results are reported in bold. Data are displayed as the mean ± SD.

Statistical analysis

The Shapiro-Wilk test was used to assess the normality of the data distribution. All the data were normally distributed. The average number of identified motor units was evaluated using independent-sample t-tests. The MVF, arm circumference, SST, CoVF, coherence, and averaged ΔF comparisons were assessed with paired sample t-tests to account for differences between related measurements (within-participant), reducing variability and improving statistical precision compared to a one-way ANOVA or independent-sample t-test, which assumes independent observations. The proportion of differences in coherence between the dominant and non-dominant limbs was calculated as the coherence ratio within each bandwidth ($[\chi-\gamma]/\chi$), where χ is the coherence for the dominant limbs whereas γ is the coherence for the non-dominant limbs. To compare limb differences in the DR_{MEAN}, DR_R, DR_P, DR_D, ISIv, absolute and relative RT and DT, motor unit ΔF, and sex differences for ΔF, mixed-effect linear regression analysis was employed to incorporate the whole sample of extracted motor units, which preserves variability within and across participants simultaneously to the greatest extent. Limb, contraction intensity, and the interaction between these were considered fixed effects, with a random intercept for each participant [e.g., RT ~ limb x intensity + (1 | Participant ID)]. Bonferroni corrections were performed to account for multiple comparisons when statistically significant. Correlations between *i*) interspike-interval variability and CoVF, *ii*) discharge rates and recruitment thresholds, *iii*) recruitment and derecruitment thresholds, and *iv*) CoVF and each coherence bandwidth were calculated using Pearson's correlation analysis. One-way ANOVAs were performed to test the difference in the *slopes* between the dominant and non-dominant sides[44]. The effect size for significant results of the t-tests was calculated using Cohen's d, whereas partial eta squared was computed for significant results of the mixed-effect analysis to estimate the proportion of variance a specific predictor explains while controlling for random effects, as previously described[45]. The statistical analyses were performed using SPSS 25.0 (IBM Corp., Armonk, NY, United States) and jamovi 2.3.28 (The jamovi project, Sydney, Australia). A $p < 0.05$ was considered statistically significant. The data are reported as the mean ± SD in the text.

Results

The distributions of the identified motor units are summarized in Table 1, whereas comparisons of the myoelectrical parameters are reported in Table 2.

Motor unit identification, MVF, and anthropometrics

A total of 703 motor units were identified after decomposition: 349 from non-dominant limbs and 354 from dominant limbs. No differences were found in the average number of identified motor units per participant across the whole sample (D, 14.75 ± 2.87; ND, 14.54 ± 3.57, $p = 0.82$), as well as at 10% MVF (D, 5.20 ± 1.38; ND, 4.75 ± 1.62, $p = 0.29$), 35% MVF (D, 5.66 ± 1.20; ND, 6.0 ± 1.79, $p = 0.45$), and 70% MVF (D, 3.87 ± 1.26; ND, 3.79 ± 0.97, $p = 0.79$). As mentioned in the methods section (*coherence estimation*), only 146 motor units were considered for the analysis at 10%MVF (73 per limb), identified in 17 participants.

Concerning the maximum mechanical output, significant differences were observed in the MVF between the dominant (283 ± 108 N) and non-dominant (257 ± 97 N, $p = 0.001$, d = 0.25) limbs, with a limb symmetry index of 91.2 ± 8.7%. No significant differences were observed in the limb circumference (D, 28.6 ± 4.41 cm; ND, 28.4 ± 4.21 cm, $p = 0.142$) or SST (D, 5.12 ± 2.67 mm; ND, 5.56 ± 2.54 mm, $p = 0.102$).

Motor unit properties

The absolute recruitment threshold was significantly higher in the dominant than in the non-dominant limbs at both 35% MVF ($p < 0.001$, $p\eta^2 = 0.07$) and 70% MVF ($p < 0.001$, $p\eta^2 = 0.12$), whereas no significant differences were found in the relative recruitment thresholds ($p > 0.05$). Similarly, the dominant limbs presented higher absolute derecruitment thresholds at 35% MVF ($p = 0.009$, $p\eta^2 = 0.03$) and 70% MVF ($p = 0.006$, $p\eta^2 = 0.05$), whereas the relative derecruitment thresholds were comparable between limbs ($p > 0.05$). DR_{MEAN} was significantly higher in motor units of dominant limbs across all contraction intensities (10% MVF, $p = 0.001$, $p\eta^2 = 0.14$; 35% MVF, $p < 0.001$, $p\eta^2 = 0.07$; 70% MVF, $p < 0.001$, $p\eta^2 = 0.13$). Additionally, motor units from the dominant muscles displayed a higher discharge rate during each ramp phase at 35% MVF (DR_R, $p < 0.001$, $p\eta^2 = 0.06$; DR_P, $p = 0.003$, $p\eta^2 = 0.05$; DR_D, $p = 0.009$, $p\eta^2 = 0.06$) and 70% MVF (DR_R, $p < 0.001$, $p\eta^2 = 0.07$; DR_P, $p < 0.001$, $p\eta^2 = 0.08$; DR_D, $p < 0.001$, $p\eta^2 = 0.06$).

Interspike interval variability and force steadiness

Motor units from both sides showed similar interspike interval variability in both the ramp contractions (35% MVF, $p = 0.764$; 70% MVF, $p = 0.483$) and sustained contractions (10% MVF, $p = 0.140$). Similarly, no differences were observed in the coefficient of variation of force during ramp contractions at 35%MVF (ND, 2.63 ± 1.15%; D, 2.50 ± 1.14%, $p = 0.589$) and 70% MVF (ND, 3.16 ± 1.34%; D, 3.07 ± 1.41%, $p = 0.705$), as well as in sustained contractions at 10% MVF (ND, 2.24 ± 0.97%; D, 1.98 ± 0.54%, $p = 0.267$). A significant (positive) association between the ISIv and the CovF% was found in both limbs at 10% MVF (ND: $r = 0.75$, $p = 0.008$; D: $r = 0.82$, $p < 0.0001$), 35% MVF (ND: $r = 0.84$, $p < 0.0001$; D: $r = 0.81$, $p < 0.0001$), and 70% MVF (ND: $r = 0.73$, $p = 0.0001$; D: $r = 0.61$, $p = 0.002$), with no differences in the slope comparison [$p > 0.05$ (Fig. 2)].

Recruitment and discharge patterns

At 35% MVF, a positive association between the recruitment and derecruitment thresholds was observed in both non-dominant ($r = 0.82 \pm 0.16$, all $p < 0.01$) and dominant ($r = 0.81 \pm 0.22$, all $p < 0.01$) limbs, with similar slopes ($p = 0.581$). Furthermore, an inverse association between the mean discharge rate and the relative recruitment threshold was observed in both non-dominant ($r = -0.77 \pm 0.25$, all $p < 0.01$) and dominant ($r = -0.68 \pm 0.26$; all $p < 0.05$) limbs, with no differences in the slope comparison ($p = 0.374$) but different intercepts ($p < 0.01$). Similarly, a positive association between the recruitment and derecruitment thresholds was observed at 70% MVF for both limbs (ND, $r = 0.75 \pm 0.23$, all $p < 0.05$; D, $r = 0.75 \pm 0.24$, $p < 0.05$ in all participants), with no significant differences in the slopes ($p = 0.746$). Both limbs also showed inverse relationships between the discharge rate and recruitment threshold (ND, $r = -0.76 \pm 0.27$; all $p < 0.01$; D, $r = -0.74 \pm 0.25$; all $p < 0.01$) with comparable slopes ($p = 0.535$) and different intercepts ($p < 0.01$).

Coherence

First, participants presented most of the coherence values above the significant threshold values (*z*-score > 1.22), with at least one coherence value above the thresholds in each analyzed bandwidth. Significant differences were found in the δ bandwidth [ND: 3.74 ± 0.66, D: 3.97 ± 0.71, $p < 0.001$, d = 1.57 (Fig. 3)], whereas no significant differences were observed in the α [ND: 1.92 ± 0.36, D: 1.97 ± 0.34, $p = 0.896$ (Fig. 3B)] and β [ND: 1.42 ± 0.25; D: 1.45 ± 0.22, $p = 0.965$ (Fig. 3C)] bandwidths. The coherence ratio revealed that the dominant limb presented ~ 14% greater values than its contralateral side in the δ-bandwidth. No significant association was found between the delta bandwidth and the CoVF for the dominant ($p = 0.403$) and non-dominant ($p = 0.429$) sides. However, significant positive correlations were observed between alpha and beta coherence with the CoVF in the dominant (α, $r = 0.70$, $p = 0.002$; β, $r = 0.80$, $p < 0.001$) and non-dominant (α, $r = 0.65$, $p = 0.003$; β, $r = 0.78$, $p = 0.001$) limbs. No significant differences were observed in the slope comparisons for each association.

Firing rate hysteresis

In the present analysis, 231 unit-wise comparisons (35% MVF, $n = 142$; 70% MVF, $n = 89$) were identified, roughly 49% of the whole sample (referring to ramps). For high-intensity contractions (70%MVF), three participants did not satisfy the requirements for comparing unit-wise and were not considered. The discharge rate hysteresis was similar between dominant and non-dominant limbs at both contraction intensities [35% MVF: ND, 2.48 ± 1.38 pps; D, 2.63 ± 1.65 pps, $p = 0.494$ (Fig. 4A); 70% MVF: ND, 2.16 ± 1.30 pps; D, 2.52 ± 1.62 pps, $p = 0.223$ (Fig. 4B)]. The mean participants' persistent inward current was also similar between dominant and non-dominant limbs at 35%MVF ($p = 0.970$) and 70%MVF ($p = 0.366$), as displayed in Fig. 5A,B. No between-limb differences were also observed in the male ($p = 0.163$) and female ($p = 0.628$) groups. Nevertheless, females presented consistently higher ΔF than males (Fig. 4C) for both the dominant (+1.18 pps, $p = 0.009$, $p\eta^2 = 0.44$) and non-dominant (+1.11 pps, $p = 0.01$, $p\eta^2 = 0.39$) limbs. Results referring to 70% MVF contractions were reported only for information completeness, as this intensity level has not been validated for estimating PICs with the paired motor unit method. Therefore, comparisons for sex differences were only performed at the 35% MVF.

Input-Output gain of motoneurons

The analysis of the input-output gain of motoneurons revealed no significant differences in the slopes calculated for the dominant and non-dominant limbs [$p = 0.763$ (Fig. 5)]. These findings indicate that, at comparable levels of synaptic input received, the motoneuronal pool transmits similar levels of neural drive to the muscles. However, this does not imply that the dominant and non-dominant limbs receive equivalent levels of common synaptic input or that their neural drive is comparable in absolute terms. Consequently, while the relationship between synaptic input and neural drive (as represented by the slopes) appears comparable, our results also indicated significant differences in the absolute values of the proportion of common inputs and the discharge

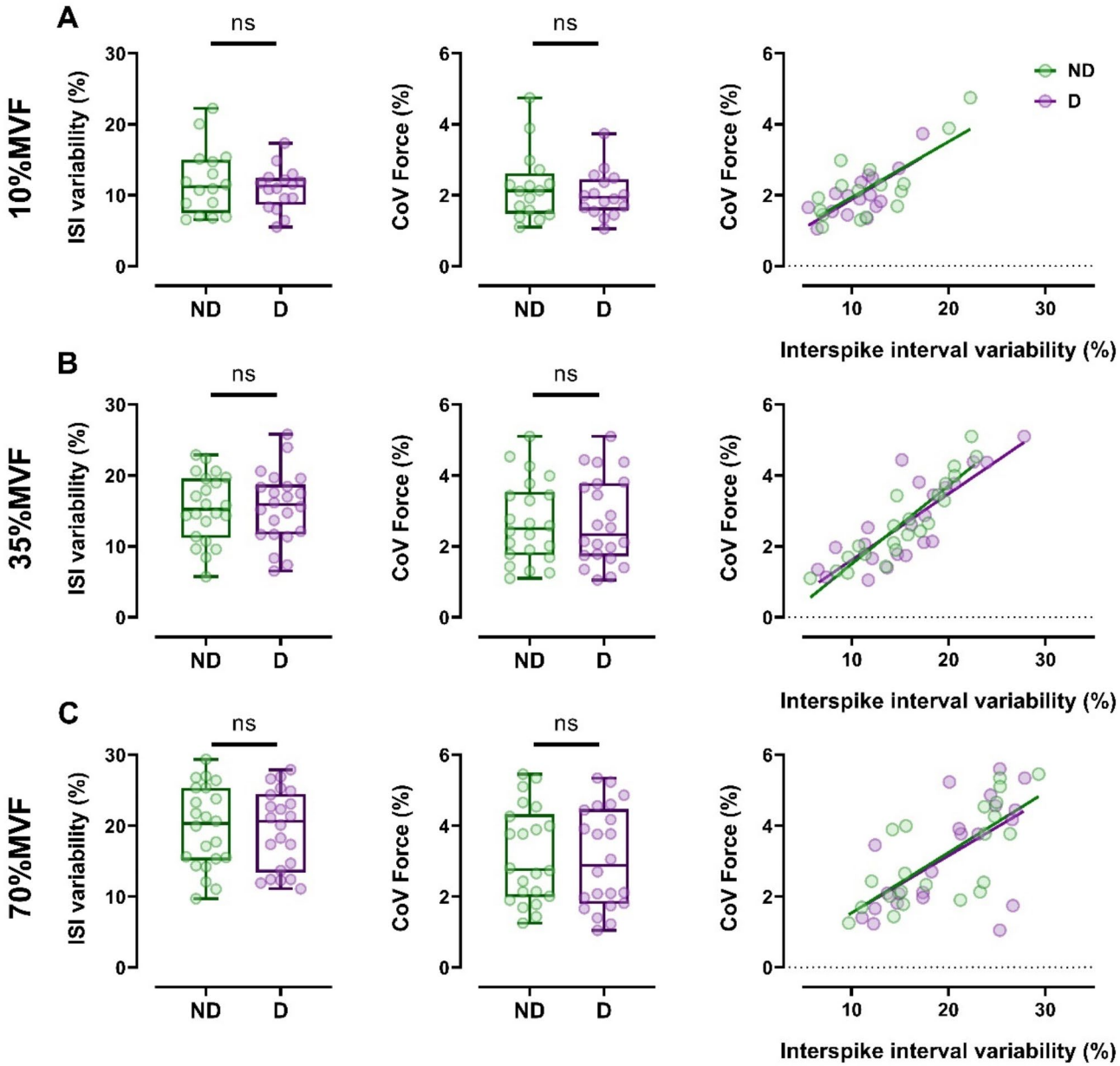

Fig. 2. Force and discharge fluctuations The interspike interval (ISI) variability and coefficient of variation (CoV) of force for both the dominant and non-dominant sides are presented using box and whisker plots at 10% MVF (**A**), 35% MVF (**B**), and 70% MVF (**C**). The association between ISI variability and the CoV of force is illustrated with a scatter plot for both limbs across all contraction intensities. Each marker represents an individual's average value. *D* dominant limbs, *ND* Non-dominant limbs.

rate (motoneuron output). Thus, the observed similarity in input-output gain should be interpreted as reflecting comparable transmission of synaptic input through neural drive[31,46].

Discussion

The main finding of this study was that greater muscle strength of dominant limbs is associated with a higher proportion of common synaptic inputs and motor unit discharge rates. Higher discharge rates do not seem to depend on intrinsic motoneuron properties, as no differences in firing rate hysteresis were observed. These results suggest that the higher discharge rate observed in dominant muscles primarily depends on the greater proportion of shared synaptic inputs to the dominant motoneuron pool, implying a higher neural drive to muscles (Fig. 6).

The dominant limbs presented greater maximal voluntary force, suggesting higher mechanical output capacity than the contralateral side (approximately + 9%), consistent with established limb-symmetry indices[1,47]. Although underlining an asymmetrical force production, our findings align with the expected differences

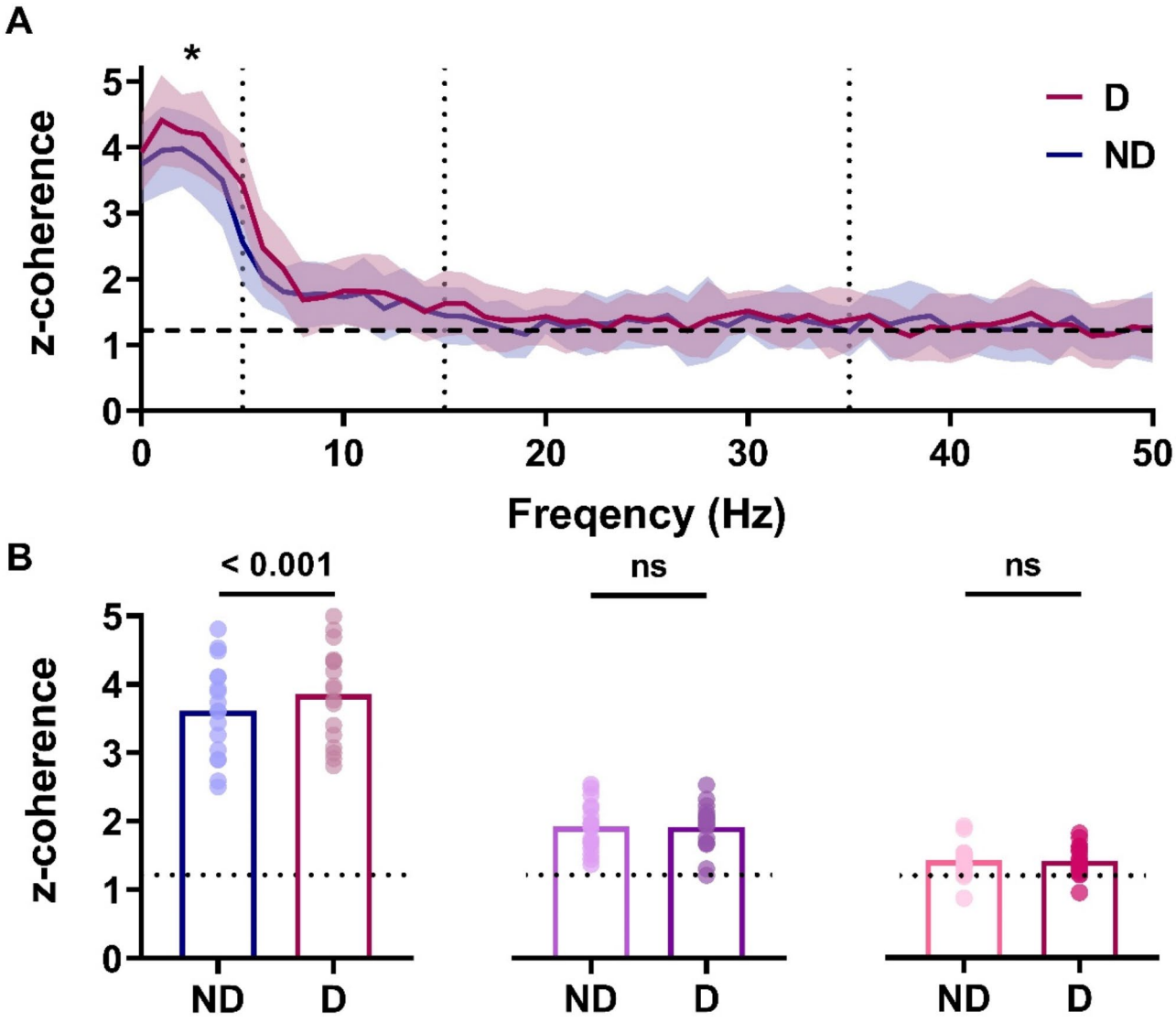

Fig. 3. Coherence analysis in the frequency domain Coherence profiles are presented as line plots across all bandwidths. The mean values are depicted as bold lines, with the shade areas within SD. The mean coherence (z-coherence) results are displayed for dominant and non-dominant sides using box plots for each bandwidth. Each marker represents a single participant's result. The rows correspond to specific bandwidth analyses: δ [0–5 Hz (**A**)], α [5–15 Hz (**B**)], β [15–35 Hz (**C**)]. *D* dominant limbs, *ND* Non-dominant limbs. The significant value is reported as a dotted line at the value of z score = 1.22 (95% confidence interval). A $p < 0.05$ was considered statistically significant.

between the dominant and non-dominant sides. Nevertheless, different neurophysiological mechanisms may explain the different extent of muscle strength observed between limbs.

First, motor units from dominant biceps brachii are activated and deactivated at a higher absolute force compared to its contralateral homologous muscle, whereas comparisons of relative recruitment and derecruitment thresholds revealed no inter-limb disparities. This evidence suggests higher absolute force at which motor units start discharging action potentials may depend on the larger maximal force output of the dominant limbs, which differs from previous research indicating greater recruitment thresholds in non-dominant muscles [FDI muscle, *iEMG, and HDsEMG*][8,9]. However, since the observed results may depend on the number (i.e., distribution) of identified units displaying specific properties[25,26,48], we characterized the activation and deactivation patterns. The positive association between the recruitment and derecruitment thresholds observed on the dominant and non-dominant sides aligns with previous studies[23,26,49], confirming no between-limb differences in the level of force at which motor units are activated relative to that at which they are deactivated. Nevertheless, the higher force levels of the dominant side implicated motor units were identified at greater absolute threshold forces, as the superimposed electrical activity of multiple motor units contributes to the increasing force output. In turn, the higher force-generating capacity of these motor units further amplifies the overall muscle force, which may result in greater contribution from the higher threshold units on the dominant side[50,51].

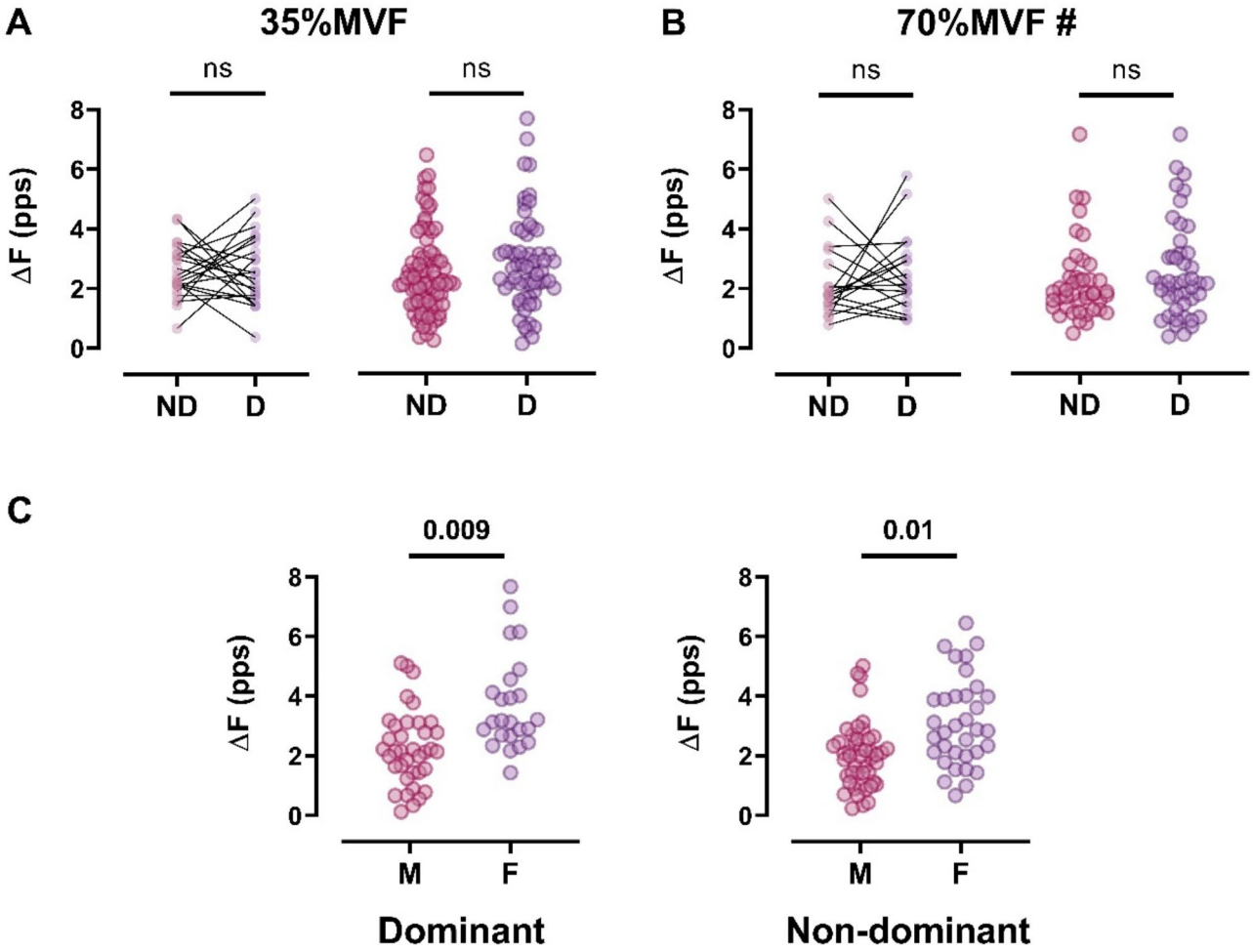

Fig. 4. Firing rate hysteresis Scatter plots were used to display the discharge rate hysteresis at 35% (**A**) and 70% MVF (**B**) as participants' mean ΔF and unit ΔF. No differences (ns) were observed in the persistent inward current amplitude. There were significant differences in male and female motor units on both sides (**C**) at 35% MVF. *D* dominant limbs, *F* Females, *M* Males, *ND* Non-dominant limbs. A $p < 0.05$ was considered statistically significant. #70% MVF contractions are not validated for calculating ΔF; data are reported for completeness of information for the whole sample and were not considered for discussion.

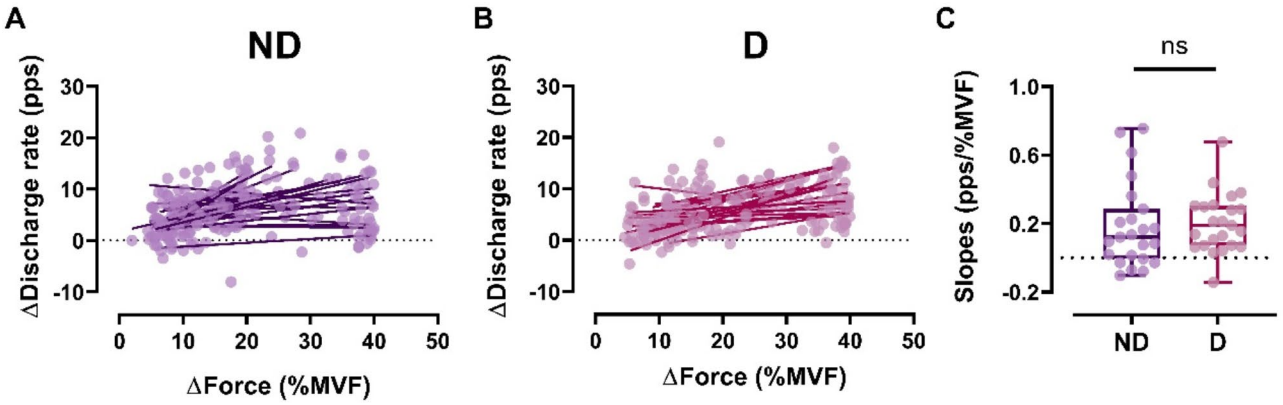

Fig. 5. Input-output gain of motoneurons Scatter plots display the associations between the gain in discharge rate and force exerted during the ramp phase [*recruitment* to *plateau*] for non-dominant (**A**) and dominant (**B**) limbs, with individual slopes. Each marker represents a single motor unit. (**C**) A box and whisker plot shows the comparison between slopes. *D* dominant limbs, *ND* non-dominant limbs.

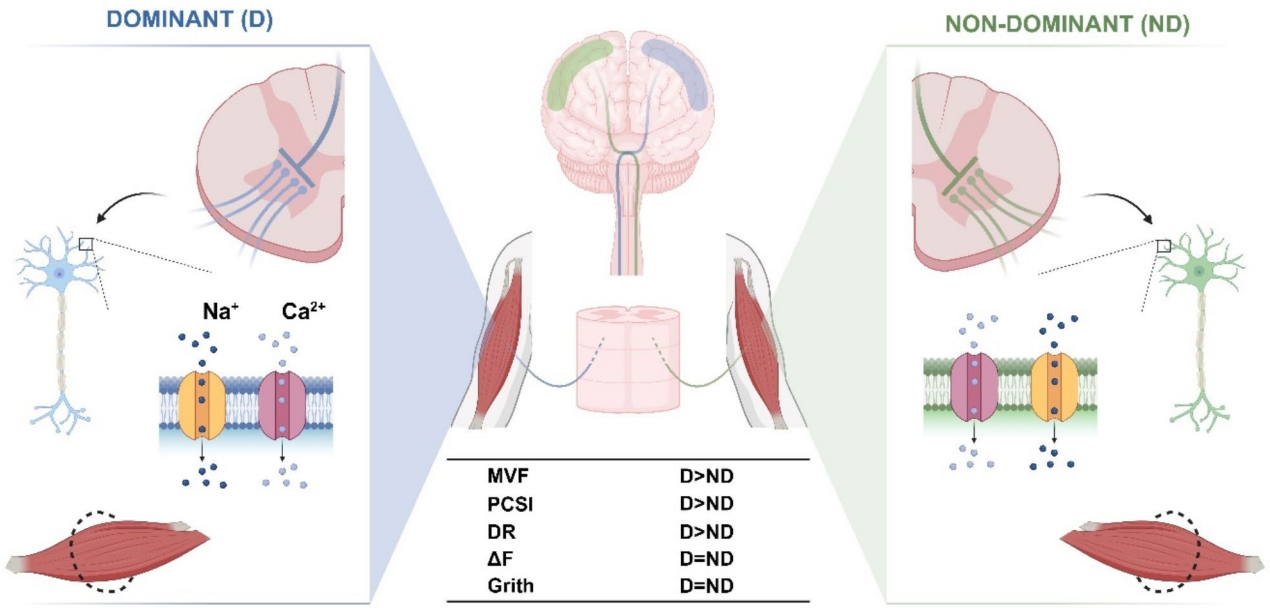

Fig. 6. Neuromuscular differences underlying limb dominance in the biceps-brachii. Dominant muscles exhibit greater maximal voluntary force (MVF) compared to the non-dominant side, together with a greater proportion of common synaptic input (PCSI) and a higher motor unit discharge rate (DR). These findings are independent of intrinsic motoneuron properties, estimated through firing rate hysteresis (ΔF), depending on the intrinsic motoneuron excitability relying on sodium and L-calcium membrane channels. This suggests that different proportions of shared common synaptic inputs primarily govern the higher neural drive to dominant muscles. The observation of similar limb circumferences (*grith*) between the dominant and non-dominant sides indicates that muscle size is not a determining factor in limb dominance.

Our results also indicate significant disparities in discharge properties between the dominant and non-dominant sides. In contrast to previous research[7,9], we found that the mean discharge rate was significantly higher in motor units from dominant muscles than the contralateral side across the three contraction intensities [10%, 35%, and 70% MVF]. Additionally, we found that the discharge rate was consistently higher in the dominant limbs across all ramp phases [recruitment, plateau, and derecruitment], implying a greater neural drive on the dominant side[46]. Nonetheless, the association between the motor unit discharge rate and the relative recruitment threshold revealed an inverse correlation in all participants, aligning with previous evidence describing similar relationships in controlled contractions[23,49]. In addition, the similar slopes but different intercepts indicate a higher neural drive delivered by the motoneuronal pool at all contraction intensities[23,49].

The interspike interval variability was comparable between the dominant and non-dominant limbs, indicating similar firing fluctuations at all contraction intensities. This finding does not support previous evidence reporting higher variability in motor units from the non-dominant side[9]. However, the influence of the analyzed muscle may imply differential fluctuations in the discharge rate [FDI versus BB], as larger muscles have been reported to display lower discharge fluctuations, plausibly leading to similar between-limb values[52]. In addition, the similar coefficient of force variation observed in our study aligns with previous evidence underlining the absence of between-limb disparities in force steadiness[11]. A significant positive association between alpha and beta coherence with the coefficient of variation of force was also observed, supporting previous research indicating a strong relationship between these variables[53,54]. Furthermore, a similar association between the ISIv and the coefficient of variation of force implies that dominant and non-dominant limbs exhibit comparable force steadiness in response to a certain fluctuation in discharge rate. These observations are supported by evidence highlighting the positive association between force and firing fluctuations[53].

Coherence analyses revealed higher δ coherence values, with up to 14% more than those observed in non-dominant limbs. Since the analysis included the same number of motor units, our results suggest that the biceps brachii on the dominant side receive a higher proportion of shared synaptic input[37], potentially explaining the observed higher neural drive[31,46]. Indeed, δ coherence is related to the *common drive*, which has been directly associated with the motoneuron output to the muscle (discharge rate), implicating a higher neural drive for force exertion[30,31,37,46]. In contrast to previous studies, which reported a lower proportion of common inputs on the dominant side during isometric rotational tasks but similar between-side coherence during isometric contractions of the FDI[13], we observed a higher level of common synaptic input. These discrepancies may be attributed to a differential distribution of common synaptic inputs across muscle groups, depending on their function and the task performed. Smaller distal muscles involved in fine motor tasks may rely on a lower proportion of common input or multiple sources of common input to allow for more flexible recruitment of motoneurons, facilitating finer motor control[14–16]. For instance, tasks such as pinching or isometric rotational

contractions require reduced common input to ensure precise control of motor unit recruitment[13]. In contrast, larger proximal muscles, such as the biceps brachii, engaged in gross motor tasks rather than finer movements, are likely to rely on greater common input. This would increase the common modulation of motor units, enhancing neural drive and force output required for such tasks[14–16]. This study is the first to compare the proportion of common synaptic input between the dominant and non-dominant biceps brachii. Further research is needed to confirm these findings across different tasks and muscle groups. Nevertheless, no significant differences were observed in the α and β bandwidths, reflecting similar common inputs from sensory afferences, sensorimotor signals, and corticomuscular integration[27,54].

Conversely to what we hypothesized, dominant and non-dominant limbs presented similar estimates of the persistent inward current, which suggests comparable motoneuron intrinsic properties[19]. Paired motor unit analysis has been broadly used for comparing estimates of the persistent inward currents[40,41] with high levels of accuracy in detecting their contribution to motoneuron intrinsic properties, even in intervention experimental designs[41]. PICs have been associated with the non-linearity behavior of the motoneuron discharge activity due to their influence on the initiation and amplification of the neural drive[19,39]. However, although we found a greater discharge rate on motor units from the dominant side, these do not seem to depend on the intrinsic properties of the motoneurons. Therefore, it is plausible that the greater discharge rate and force output observed in the dominant limbs primarily depend on the proportion of common synaptic inputs rather than different intrinsic properties of motoneurons innervating muscles. Furthermore, our results support that females present higher PICs than males[20], which we confirm to be higher in both the dominant and non-dominant limbs. These findings align with previous results indicating greater motor unit discharge rate in female individuals in low-contraction intensities[23], thereby implicating the strict relationship between the intrinsic threshold properties of motoneurons and their resulting discharge rate[19,20,40,50]. Nevertheless, when males and females were analyzed separately, the dominant and non-dominant biceps brachii showed similar estimates of persistent inward currents, indicating comparable intrinsic motoneuron properties both across the entire sample and within each sex.

The similar PIC estimates between the dominant and non-dominant sides suggest that motoneurons on both sides similarly amplify synaptic input, resulting in a comparable neural drive when equivalent synaptic input is delivered to the motoneuronal pools[19,31,55]. To investigate this, we estimated the input-output gain across the motoneuronal pool as a measure of responsiveness to synaptic input[10,28,29]. Our findings revealed that the relationship between estimated synaptic input and motoneuronal output (discharge rate) was consistent across sides. These results do not indicate equivalent levels of common synaptic input or neural drive between the dominant and non-dominant limbs. Instead, the similar slopes reflect comparable modulation of motoneuronal responses to synaptic input[31,46], with greater neural drive to muscles likely dependent on a higher proportion of common inputs on the dominant side. This finding is supported by previous evidence referring to the motoneuronal pool as a spatial filter, amplifying shared components of synaptic input while suppressing independent noise[46], thereby transmitting correlated signals to muscles as neural drive[16,30,31]. Together, these observations suggest that the greater muscle force observed on the dominant side is associated with a higher proportion of common synaptic input. Although the discharge behavior of motor units is non-linear, the estimation of the input-output gain can provide meaningful information once a comparable contribution from the intrinsic properties of the motoneurons is confirmed[19,50].

Even though it is untypical to observe different muscle compositions and myosin-chain expression between dominant and non-dominant limbs within the same individual[56,57], as well as in the contractile properties in both the lower and upper limbs[58–60], the absence of direct muscle biopsy measurements prevents us from asserting that muscle properties are not involved in the dominance of one limb over the other, even at comparable muscle size.

In conclusion, our findings demonstrate that dominant muscles presented greater force output, accompanied by a higher proportion of common synaptic inputs to motoneurons and higher neural drive to muscles. Importantly, this higher neural drive is not attributable to differences in intrinsic motoneuron properties, as estimates of the persistent inward currents were comparable between dominant and non-dominant limbs. Furthermore, the analysis of the input-output function suggests that motoneurons generate a similar output for a certain level of synaptic input received from the pool on both sides. However, the dominant side receives a greater proportion of common synaptic input, leading to a higher neural drive to muscles, which implies greater maximal voluntary force. These findings highlight the role of the proportion of common synaptic input in driving superior motor output in the dominant limbs, which is independent of intrinsic motoneuron characteristics.

Data availability

The data supporting the findings of this study are available upon reasonable request from the corresponding author.

Received: 23 October 2024; Accepted: 3 March 2025
Published online: 10 March 2025

References

1. McGrath, T. M. et al. The effect of limb dominance on lower limb functional performance—a systematic review. *J. Sports Sci.* **34**, 289–302 (2016).
2. Semmler, J. G. & Nordstrom, M. A. Influence of handedness on motor unit discharge properties and force tremor. *Exp. Brain Res.* **104**, 115–125 (1995).
3. Semmler, J. G. & Nordstrom, M. A. Hemispheric differences in motor cortex excitability during a simple index finger abduction task in humans. *J. Neurophysiol.* **79**, 1246–1254 (1998).

4. Madarshahian, S. & Latash, M. L. Effects of hand muscle function and dominance on intra-muscle synergies. *Hum. Mov. Sci.* **82**, (2022).
5. Bernardi, M. et al. Force generation performance and motor unit recruitment strategy in muscles of contralateral limbs. *J. Electromyogr. Kinesiol.* **9**, 121–130 (1999).
6. Krzysztofik, M. et al. A comparison of muscle activity of the dominant and non-dominant side of the body during low versus high loaded bench press exercise performed to muscular failure. *J. Electromyogr. Kinesiol.* **56**, (2021).
7. Petrovic, I. et al. Leg dominance does not influence maximal force, force steadiness, or motor unit discharge characteristics. *Med. Sci. Sports Exerc.* **54**, 1278–1287 (2022).
8. Nishikawa, Y. et al. Sex differences in laterality of motor unit firing behavior of the first dorsal interosseous muscle in strength-matched healthy young males and females. *Eur. J. Appl. Physiol.* https://doi.org/10.1007/s00421-024-05420-7 (2024).
9. Adam, A., De Luca, C. J. & Erim, Z. Hand dominance and motor unit firing behavior. *J. Neurophysiol.* **80**, 1373–1382 (1998).
10. Petrovic, I. et al. Footedness but not dominance influences force steadiness during isometric dorsiflexion in young men. *J. Electromyogr. Kinesiol.* **73**, (2023).
11. Willems, M. E. T. & Ponte, J. P. G. Divergent muscle fatigue during unilateral isometric contractions of dominant and non-dominant quadriceps. *J. Sci. Med. Sport*. **16**, (2013).
12. Ojha, A., Alderink, G. & Rhodes, S. Coherence between electromyographic signals of anterior tibialis, Soleus, and gastrocnemius during standing balance tasks. *Front. Hum. Neurosci.* **17**, (2023).
13. Maillet, J., Avrillon, S., Nordez, A., Rossi, J. & Hug, F. Handedness is associated with less common input to spinal motor neurons innervating different hand muscles. *J. Neurophysiol.* **128**, 778–789 (2022).
14. Rossato, J. et al. Less common synaptic input between muscles from the same group allows for more flexible coordination strategies during a fatiguing task. *J. Neurophysiol.* **127**, (2022).
15. Del Vecchio, A. et al. The forces generated by agonist muscles during isometric contractions arise from motor unit synergies. *J. Neurosci.* **43**, 2860–2873 (2023).
16. Hug, F., Avrillon, S., Ibáñez, J. & Farina, D. Common synaptic input, synergies and size principle: Control of spinal motor neurons for movement generation. *J. Physiol.*. **601**. https://doi.org/10.1113/JP283698 (2023).
17. Kelly, R., Mizelle, J. C. & Wheaton, L. A. Distinctive laterality of neural networks supporting action Understanding in left- and right-handed individuals: an EEG coherence study. *Neuropsychologia*. **75**, (2015).
18. Sainburg, R. L. & Kalakanis, D. Differences in control of limb dynamics during dominant and nondominant arm reaching. *J. Neurophysiol.* **83**, (2000).
19. Binder, M. D., Powers, R. K. & Heckman, C. J. Nonlinear input-output functions of motoneurons. *Physiology*. **35**, 31–39 (2020).
20. Jenz, S. T. et al. Estimates of persistent inward currents in lower limb motoneurons are larger in females than in males. *J. Neurophysiol.* **129**, 1322–1333 (2023).
21. Elliott-Sale, K. J. et al. The effects of oral contraceptives on exercise performance in women: A systematic review and Meta-analysis. *Sports Med.* **50**, (2020).
22. Oldfield, R. C. The assessment and analysis of handedness: the Edinburgh inventory. *Neuropsychologia*. **9**, (1971).
23. Lecce, E., Conti, A., Nuccio, S., Felici, F. & Bazzucchi, I. Characterising sex-related differences in lower- and higher-threshold motor unit behaviour through high-density surface electromyography. *Exp. Physiol.* **109**, 1–13 (2024).
24. Lecce, E. et al. Exerting force at the maximal speed drives the increase in power output in elite athletes after 4 weeks of resistance training. *Eur. J. Appl. Physiol.* https://doi.org/10.1007/s00421-024-05604-1 (2024).
25. Holobar, A. & Zazula, D. Multichannel blind source separation using convolution kernel compensation. *IEEE Trans. Signal Process.* **55**, 4487–4496 (2007).
26. Del Vecchio, A. et al. Tutorial: analysis of motor unit discharge characteristics from high-density surface EMG signals. *J. Electromyogr. Kinesiol.* **53**, (2020).
27. Lecce, E. et al. Sensorimotor integration is affected by acute whole-body vibration: a coherence study. *Front. Physiol.* **14**, (2023).
28. Del Vecchio, A. et al. The increase in muscle force after 4 weeks of strength training is mediated by adaptations in motor unit recruitment and rate coding. *J. Physiol.* **597**, 1873–1887 (2019).
29. Martinez-Valdes, E., Negro, F., Farina, D. & Fallah, D. Divergent response of low- versus high-threshold motor units to experimental muscle pain. *J. Physiol.* 2093–2108 (2020).
30. Farina, D., Negro, F., Muceli, S. & Enoka, R. M. Principles of motor unit physiology evolve with advances in technology. *Physiology* **31**, 83–94 (2016).
31. Negro, F. & Farina, D. Linear transmission of cortical oscillations to the neural drive to muscles is mediated by common projections to populations of motoneurons in humans. *J. Physiol.* **589**, (2011).
32. Lecce, E. et al. Cross-education: motor unit adaptations mediate the strength increase in non-trained muscles following 8 weeks of unilateral resistance training. *Front. Physiol.* **15**, (2025).
33. Del Vecchio, A. et al. Spinal motoneurons of the human newborn are highly synchronized during leg movements. *Sci. Adv.* **6**, (2020).
34. De La Rocha, J., Doiron, B., Shea-Brown, E., Josić, K. & Reyes, A. Correlation between neural spike trains increases with firing rate. *Nature*. **448**, (2007).
35. Avrillon, S. et al. Individual differences in the neural strategies to control the lateral and medial head of the quadriceps during a mechanically constrained task. *J. Appl. Physiol.* **130**, (2021).
36. Nuccio, S. et al. Neuroplastic alterations in common synaptic inputs and synergistic motor unit clusters controlling the Vastii muscles of individuals with ACL reconstruction. *J. Appl. Physiol.* **137**, 835–847 (2024).
37. Castronovo, A. M., Negro, F., Conforto, S. & Farina, D. The proportion of common synaptic input to motor neurons increases with an increase in net excitatory input. *J. Appl. Physiol.* **119**, 1337–1346 (2015).
38. Negro, F. & Farina, D. Factors influencing the estimates of correlation between motor unit activities in humans. *PLoS One*. **7**, (2012).
39. Gorassini, M. A., Bennett, D. J. & Yang, J. F. Self-sustained firing of human motor units. *Neurosci. Lett.* **247**, 13–16 (1998).
40. Orssatto, L. B. R. et al. Estimates of persistent inward currents increase with the level of voluntary drive in low-threshold motor units of plantar flexor muscles. *J. Neurophysiol.* **125**, 1746–1754 (2021).
41. Goodlich, B. I., Vecchio, D., Horan, A., Kavanagh, J. J. & S. A. & Blockade of 5-HT 2 receptors suppresses motor unit firing and estimates of persistent inward currents during voluntary muscle contraction in humans key points. *J. Physiol.* **601**, 1121–1138 (2023).
42. Revill, A. L. & Fuglevand, A. J. Effects of persistent inward currents, accommodation, and adaptation on motor unit behavior: a simulation study. *J. Neurophysiol.* **106**, 1467–1479 (2011).
43. Mesquita, R. N. O. et al. Effects of jaw clenching and mental stress on persistent inward currents estimated by two different methods. *Eur. J. Neurosci.* **58**, 4011–4033 (2023).
44. Andrade, J. M. & Estévez-Pérez, M. G. Statistical comparison of the slopes of two regression lines: A tutorial. *Anal. Chim. Acta*. **838**, 1–12 (2014).
45. Correll, J., Mellinger, C. & Pedersen, E. J. Flexible approaches for estimating partial Eta squared in mixed-effects models with crossed random factors. *Behav. Res. Methods*. **54**, 1626–1642 (2022).
46. Farina, D., Negro, F. & Dideriksen, J. L. The effective neural drive to muscles is the common synaptic input to motor neurons. *J. Physiol.* **592**, 3427–3441 (2014).

47. Jones, P. A. & Bampouras, T. M. A comparison of isokinetic and functional methods of assessing bilateral strength imbalance. *J. Strength. Cond. Res.* **24**, (2010).
48. Holobar, A. & Farina, D. Blind source identification from the multichannel surface electromyogram. *Physiol. Meas.* **35**, 143–165 (2014).
49. De Luca, C. & Hostage, E. Relationship between firing rate and recruitment threshold of motoneurons in voluntary isometric contractions. *J. Neurophysiol.* **104**, 1034–1046 (2010).
50. Heckman, C. J. & Enoka, R. M. Motor unit. *Compr. Physiol.* **2**, 2629–2682 (2012).
51. Enoka, R. M. & Duchateau, J. Inappropriate interpretation of surface EMG signals and muscle fiber characteristics impedes understanding of the control of neuromuscular function. *J. Appl. Physiol.* **119**. https://doi.org/10.1152/japplphysiol.00280.2015 (2015).
52. Hamilton, A. F. D. C., Jones, K. E. & Wolpert, D. M. The scaling of motor noise with muscle strength and motor unit number in humans. *Exp. Brain Res.* **157**, (2004).
53. Enoka, R. M. & Farina, D. Force steadiness: from motor units to voluntary actions. *Physiology*. **36**, (2021).
54. Ushiyama, J., Yamada, J., Liu, M. & Ushiba, J. Individual difference in β-band corticomuscular coherence and its relation to force steadiness during isometric voluntary ankle dorsiflexion in healthy humans. *Clin. Neurophysiol.* **128**, 303–311 (2017).
55. Powers, R. K. & Heckman, C. J. Contribution of intrinsic motoneuron properties to discharge hysteresis and its Estimation based on paired motor unit recordings: a simulation study. *J. Neurophysiol.* **114**, 184–198 (2015).
56. Mandroukas, A. et al. Myosin heavy chain isoform composition in the deltoid and Vastus lateralis muscles of elite handball players. *J. Sports Sci.* **38**, 2390–2395 (2020).
57. Mavidis, A. et al. Morphology of the deltoid muscles in elite tennis players. *J. Sports Sci.* **25**, 1501–1506 (2007).
58. Parmar, A., Scott, M., Brand, C. & Jones, T. W. An assessment of the contractile properties of the shoulder musculature in elite volleyball players using tensiomyography. *Int. J. Sports Phys. Ther.* **15**, 1099–1109 (2020).
59. Mooney, K., Warner, M. & Stokes, M. Symmetry and within-session reliability of mechanical properties of biceps brachii muscles in healthy young adult males using the MyotonPRO device. *Work Pap. Health Sci.* **1**, (2013).
60. Jones, A. et al. Muscle contractile properties of professional soccer players according to playing position and limb dominance. *J. Elite Sport Perform.* **3**, (2023).

Author contributions

All authors participated equally in document drafting, data collection, and analysis. E.L., A.D.V., and I.B. conceived the work and made the figures; all the authors revised the final version. All the authors have read and approved the final version of this manuscript and agree to be accountable for all aspects of the work, ensuring that questions related to the accuracy or integrity of any part of the work are appropriately investigated and resolved. All persons designated as authors qualify for authorship, and all those who qualify are listed.

Funding

The exercise physiology laboratory of the University of 'Foro Italico' needed no additional funding for the present study. The present work was supported by grant [CDR2.PNRR2023-DM737/2021].

Declarations

Competing interests

The authors declare no competing interests.

Additional information

Correspondence and requests for materials should be addressed to I.B.

Reprints and permissions information is available at www.nature.com/reprints.

Publisher's note Springer Nature remains neutral with regard to jurisdictional claims in published maps and institutional affiliations.